

LA-UR-03-3853
nucl-th/0306043

High strangeness dibaryons in the extended quark delocalization, color screening model

Hourong Pang

Department of Physics, Nanjing University, Nanjing, 210093, P. R. China;

Institute of Theoretical Physics, Chinese Academy of Sciences, Beijing, 100080, China

Jialun Ping

Department of Physics, Nanjing Normal University, Nanjing, 210097, P.R. China;

Center for Theoretical Physics, Nanjing University, Nanjing, 210093, P.R. China

Fan Wang

Center for Theoretical Physics and Department of Physics,

Nanjing University, Nanjing, 210093, P. R. China

T. Goldman

Theoretical Division, Los Alamos National Laboratory, Los Alamos, NM 87545, USA

Enguang Zhao

Institute of Theoretical Physics, Chinese Academy of Science, Beijing, 100080, China

Abstract

Dibaryon candidates with strangeness $S = -2, -3, -4, -5, -6$ are studied in terms of the extended quark delocalization and color screening model. The results show that there are only few promising low lying dibaryon states: The H and di- Ω may be marginally strong interaction stable but model uncertainties are too large to allow any definitive statement; the $SIJ = -3, 1/2, 2$ $N\Omega$ state is $62 MeV$ lower than the $N\Omega$ threshold and $24 MeV$ lower than the $\Lambda\Xi\pi$ threshold. In addition, we study the mechanisms of effective intermediate range attraction, σ meson exchange and the kinetic energy reduction due to quark delocalization.

PACS numbers: 12.39.-x, 14.20.Pt, 13.75.Cs

I. INTRODUCTION

One of the most remarkable achievements of theoretical physics in the past thirty years is the establishment and development of the fundamental theory of strong interaction – quantum chromodynamics (QCD). Perturbative QCD has been verified by high energy experiments. However, the low energy physics of QCD, like hadron structure, hadron interactions and the structure of exotic quark-gluon systems, are much harder to calculate directly from QCD. One needs effective theories and phenomenological models in these cases.

Borrowing the idea of quasiparticles from condensed matter and nuclear physics, one can approximately transform the complicated interactions between current quarks into dynamic properties of quasiparticles and what is left to be studied is the residual interactions between quasiparticles. One of the quasiparticles in QCD is the constituent quark. How the current quark is dressed to become a constituent quark is still a theoretical challenge; various effective theories[1, 2, 3] have been developed to derive constituent quarks from QCD. The common point of view is that the dynamical generation of the constituent quark mass is closely related to spontaneous chiral symmetry breaking initiated by the formation of a $q\bar{q}$ condensate in the QCD vacuum.

The constituent quark model has been quite successful in understanding hadron spectroscopy and hadron interactions even though we have not yet derived the constituent quark model directly from QCD. There are also various versions of the constituent quark model based on different effective degrees of freedom. De Rujula, Georgi and Glashow[4] first put forward a quark-gluon coupling model based on the constituent quark and gluon effective degrees of freedom. Isgur obtained a good description of hadron spectroscopy based on this model[5]. However, extension of this model to baryon interactions does not describe the nucleon-nucleon intermediate and long range interaction.

One modification studied is the addition of Goldstone boson exchange on the quark level[6, 7, 8, 9], in which the short-range part of the interaction is described by the quark-gluon degrees of freedom and the medium and long-range parts are attributed to meson-exchange. This quark gluon-meson exchange hybrid model achieves a quantitative fit of the nucleon-nucleon (NN) and nucleon-hyperon (NY) scattering data.

A different modification of the De Rujula-Georgi-Glashow-Isgur (RGGI) model, the quark delocalization and color screening model (QDCSM)[10], has also been suggested. It main-

tains the Isgur Hamiltonian for single hadrons but modifies it for baryon-baryon (BB) interactions with two new ingredients.

First, the two center single quark orbital wave function (WF) used in the quark cluster model is replaced by a delocalized quark orbital WF. The introduction of quark delocalization can be viewed either as taking into account the contribution of excited configurations or the distortion of each individual baryon due to their mutual interaction. This straightforward method enlarges the variational Hilbert space. Its advantage is that it permits the six-quark system to choose a more favorable configuration through its own dynamics and while maintaining a tolerable level of computational complexity.

Second, a different parametrization of the confinement interaction is assumed, in which the usual quadratic confinement and a color-screened quadratic confinement are used to parameterize the two body matrix elements of different quark orbits. The introduction of this parametrization is aimed at taking into account some of the nonlinear, nonperturbative properties of QCD which can not be described by two-body quark-quark interactions in multiquark systems, such as the three gluon interaction and the three body instanton interaction.

The QDCSM not only justifies the view of a nucleus as, approximately, a collection of nucleons rather than a single big bag with 3A quarks, but it also explains the long standing fact that the nuclear force and molecular forces are similar except for the obvious energy and length scale differences. It is also the model which requires the fewest adjustable parameters to fit the existing BB interaction data[10, 11, 12, 13, 14, 15, 16].

There have been debates on which constituent quark model and which effective degrees of freedom are best to use for hadron structure and interaction studies[17, 18, 19, 20, 21]. In our phenomenological study of BB interactions with three different constituent quark models, we found that even though the QDCSM and the other two models appear to be quite different, they give similar BB interactions in 44 of the 64 lowest BB channels consisting of octet and decuplet baryons[14]. A preliminary analysis of the origin of this surprising similarity has been produced[22]. This result also implies that quark delocalization and color screening, working together, do provide the intermediate range attraction described by meson exchange in other models. On the other hand, the different models do give characteristically different results in some channels. For example, the QDCSM predicts a strong attraction in the $I=0$, $J=3$ channel, producing a dibaryon resonance, d^* , in this channel, while the quark gluon-

meson exchange hybrid model predicts a strong attraction in the $I=0, J=0 \Omega\Omega$ channel, implying the existence of a strong interaction stable di- Ω . One can not expect scattering data to become available in these channels to test these model predictions, but the dibaryon states should be detectable to provide a check on whether these model predictions are realistic.

Study of dibaryon states not only checks constituent quark models but also searches for the new hadronic matter. The H particle has been assumed to be a six quark system from the very beginning[23] and has been both a theoretical and experimental topic for a long time. The $S=0, J^p = 0^-$ d' dibaryon was assumed to be a $NN\pi$ system and was a hot topic in the 1990's[13, 24]. We showed that the $S = 0, I = 0, J = 3$ d^* [10, 14, 15, 25, 26, 27, 28] is a tightly bound six quark system rather than a loosely bound nuclear-like system of two Δ 's. An $S = -3, I = 1/2, J = 2$ $N\Omega$ state was proposed as a high strangeness dibaryon candidate[29]. Kopeliovich predicted high strangeness dibaryons, such as the di- Ω with $S = -6$, using the flavor SU(3) Skyrmion model[30], and Zhang suggested searching for the di- Ω in ultrarelativistic heavy ion collisions[31]. Lomon predicted a deuteron-like dibaryon resonance using R-matrix theory[32] and measurements at Saclay seem to offer experimental support[33] for its existence.

In this paper, we calculate promising dibaryons with strangeness $S = -2, -3, -4, -5$ using the extended quark-delocalization color-screening model to provide another reference spectrum for strange dibaryons and a possible further check of constituent quark models. The SIJ=003 d^* and -600 di- Ω dibaryons, which we considered previously, are included in the discussion to demonstrate the differences between the predictions of the extended QDCSM and other quark models.

The extended QDCSM is briefly introduced in Section II. In Section III, we present our results. We discuss these results further in Section IV and conclude in Section V.

II. BRIEF DESCRIPTION OF THE EXTENDED QDCSM

The QDCSM was put forward in the early 90's. Details can be found in Refs.[10, 26, 28]. Although the intermediate range attraction of the NN interaction is reproduced by the combination of quark delocalization and color screening, the effect of the long-range pion tail is missing in the QDCSM. Recently, the extended QDCSM was developed[15],

which incorporates this long-range tail by adding π -exchange with a short-range cutoff. The extended QDCSM not only reproduces the properties of the deuteron well, but also improves agreement with NN scattering data as compared to previous work[16].

The Hamiltonian of the extended QDCSM, wave functions and the necessary equations used in the current calculation are given below. Here we do not take into account the effect of any tensor forces. The details of the resonating-group method (RGM) have been presented in Refs.[28, 34].

The Hamiltonian for the 3-quark system is the same as the usual quark potential model, the Isgur model. For the six-quark system, it is assumed to be

$$\begin{aligned}
H_6 &= \sum_{i=1}^6 \left(m_i + \frac{p_i^2}{2m_i} \right) - T_{CM} + \sum_{i < j=1}^6 [V_{conf}(r_{ij}) + V_G(r_{ij}) + V_\pi(r_{ij})], \\
V_G(r_{ij}) &= \alpha_s \frac{\vec{\lambda}_i \cdot \vec{\lambda}_j}{4} \left[\frac{1}{r_{ij}} - \frac{\pi}{2} \delta(r_{ij}) \left(\frac{1}{m_i^2} + \frac{1}{m_j^2} + \frac{4\vec{\sigma}_i \cdot \vec{\sigma}_j}{3m_i m_j} \right) \right], \\
V_\pi(r_{ij}) &= \theta(r - r_0) \frac{g_{qq\pi}^2}{4\pi} \frac{\mu_\pi^2}{12m_q^2} \frac{1}{r_{ij}} e^{-\mu_\pi r_{ij}} \vec{\sigma}_i \cdot \vec{\sigma}_j \vec{\tau}_i \cdot \vec{\tau}_j, \\
V_{conf}(r_{ij}) &= -a_c \vec{\lambda}_i \cdot \vec{\lambda}_j \begin{cases} r_{ij}^2 & \text{if } i, j \text{ occur in the same baryon orbit,} \\ \frac{1-e^{-\mu r_{ij}^2}}{\mu} & \text{if } i, j \text{ occur in different baryon orbits,} \end{cases} \\
\theta(r_{ij} - r_0) &= \begin{cases} 0 & r_{ij} < r_0, \\ 1 & \text{otherwise,} \end{cases}
\end{aligned} \tag{1}$$

where r_0 is the short range cutoff for pion exchange between quarks, all the symbols have their usual meaning, and the confinement potential $V_{conf}(r_{ij})$ has been discussed in Refs.[15, 28].

The pion potential, $V_\pi(r_{ij})$, affects only the u and d quarks. We take these to have a common mass, $m_q = m_d = m_u$, ignoring isospin breaking effects as they are small on the scale of interest here.

The quark wave function in a given nucleon (orbit) relative to a reference center (defined by \vec{S}) is taken to have a Gaussian form characterized by a size parameter, b ,

$$\phi(\vec{r} - \vec{S}) = \left(\frac{1}{\pi b^2} \right)^{3/4} e^{-\frac{1}{2b^2}(\vec{r} - \vec{S})^2}. \tag{2}$$

The values of m_q , m_s , b , α_s and a_c are determined by reproducing the $N - \Delta$ mass difference, the nucleon mass, a hyperon mass and by requiring a stability condition. The quark-pion coupling constant $g_{qq\pi}$ is obtained from the nucleon-pion coupling constant by a

slight ($< 10\%$) correction to the classic symmetry relation, viz.,

$$\frac{g_{NN\pi}^2}{4\pi} = (M_N/m_q)^2 \left(\frac{5}{3}\right)^2 \frac{g_{qq\pi}^2}{4\pi} e^{\mu_\pi^2 b^2/2} \quad (3)$$

where M_N is the nucleon mass and the last factor provides the correction due to the extent of the quark wavefunction in the nucleon. The color screening parameter, μ , has been determined by matching our calculation to the mass of the deuteron. All of the parameters are listed in Table I.

Table I: Model Parameters

$m_q, m_s(\text{MeV})$	$b(\text{fm})$	$a_c(\text{MeV} \cdot \text{fm}^{-2})$	α_s	$g_{qq\pi}$	$r_0(\text{fm})$	$\mu(\text{fm}^{-2})$
313, 634	0.6015	25.14	1.5585	0.592	0.8	0.85

The model masses of all octet and decuplet baryons are listed in Table II.

Table II: Single Baryon Masses in Units of MeV

	N	Σ	Λ	Ξ	Δ	Σ^*	Ξ^*	Ω
model	939.0	1210.6	1113.6	1350.0	1232.0	1358.1	1497.5	1650.1
expt.	939	1193	1116	1318	1232	1385	1533	1672

We use the resonating group method to carry out a dynamical calculation. Introducing the Gaussian functions with different reference centers S_i $i=1\dots n$, which play the role of generating coordinates in this formalism, to expand the relative motion wave function of the two quark clusters, we have

$$\chi(\vec{R}) = \left(\frac{3}{2\pi b^2}\right)^{3/4} \sum_i C_i e^{-\frac{3}{4}(\vec{R}-\vec{S}_i)^2/b^2}.$$

In principle, any set of base wave functions can be used to expand the relative motion wave function. The choice of a Gaussian with the same size parameter, b , as the single quark wave function given in Eq.(2), however, allows us to rewrite the resonating group wave function as a product of single quark wave functions; (see Eq.(4) below). This cluster wave function (physical basis) can be expressed in terms of the symmetry basis, classified by the symmetry properties, in a group chain which in turn allows the use of group theory methods to simplify the calculation of the matrix elements of the six quark Hamiltonian. In our calculations, we typically use 12 Gaussian functions to expand the relative motion wave function over the range 0-8 fm. For a few channels, such as the deuteron, 20 Gaussian functions are used to extend the range to 12 fm.

After including the wave function for the center-of-mass motion, the ansatz for the two-cluster wave function used in the RGM can be written as

$$\Psi_{6q} = \mathcal{A} \sum_k \sum_{i=1}^n C_{k,i} \int d\Omega_{S_i} \prod_{\alpha=1}^3 \psi_R(\vec{r}_\alpha, \vec{S}_i, \epsilon) \prod_{\beta=4}^6 \psi_L(\vec{r}_\beta, \vec{S}_i, \epsilon) [\eta_{I_{1k}S_{1k}}(B_{1k}) \eta_{I_{2k}S_{2k}}(B_{2k})]^{I,J=S} [\chi_c(B_1) \chi_c(B_2)]^{[\sigma]}, \quad (4)$$

where k is the channel index. For example, for $SIJ = -2, 0, 0$, we have $k = 1, 2, 3, 4$, corresponding to the channels $\Lambda\Lambda, N\Xi, \Sigma\Sigma$ and $\Sigma^*\Sigma^*$.

The delocalized orbital wavefunctions, $\psi_R(\vec{r}, \vec{S}_i, \epsilon)$ and $\psi_L(\vec{r}, \vec{S}_i, \epsilon)$, are given by

$$\begin{aligned} \psi_R(\vec{r}, \vec{S}_i, \epsilon) &= \frac{1}{N(\epsilon)} \left(\phi(\vec{r} - \frac{\vec{S}_i}{2}) + \epsilon \phi(\vec{r} + \frac{\vec{S}_i}{2}) \right), \\ \psi_L(\vec{r}, \vec{S}_i, \epsilon) &= \frac{1}{N(\epsilon)} \left(\phi(\vec{r} + \frac{\vec{S}_i}{2}) + \epsilon \phi(\vec{r} - \frac{\vec{S}_i}{2}) \right), \\ N(\epsilon) &= \sqrt{1 + \epsilon^2 + 2\epsilon e^{-S_i^2/4b^2}}, \end{aligned} \quad (5)$$

where $\phi(\vec{r} - \frac{\vec{S}_i}{2})$ and $\phi(\vec{r} + \frac{\vec{S}_i}{2})$ are the single-particle Gaussian quark wave functions referred to above in Eq.(2), with different reference centers $\frac{\vec{S}_i}{2}$ and $-\frac{\vec{S}_i}{2}$, respectively. The delocalization parameter, ϵ , is determined by the dynamics of the quark system rather than being treated as an adjustable parameter.

The initial RGM equation is

$$\int H(\vec{R}, \vec{R}') \chi(\vec{R}') d\vec{R}' = E \int N(\vec{R}, \vec{R}') \chi(\vec{R}') d\vec{R}'. \quad (6)$$

With the above ansatz, the RGM Eq.(6) is converted into an algebraic eigenvalue equation,

$$\sum_{j,k'} C_{j,k'} H_{i,j}^{k,k'} = E \sum_j C_{j,k} N_{i,j}^k, \quad (7)$$

where $N_{i,j}^k, H_{i,j}^{k,k'}$ are the wave function overlaps and Hamiltonian matrix elements, respectively, obtained for the wave functions of Eq.(4).

III. RESULTS

Previously, we chose the di- Ω as an example to study whether or not our model results were sensitive to the meson-exchange cut-off parameter, r_0 , and the result demonstrates that they are not[35]. Hence, we consider it sufficient to calculate six-quark systems of different

strangeness, $S = -2, -3, -4, -5$, with a representative cutoff value of $r_0 = 0.8 fm$. Table III displays the masses (in MeV) calculated for the strange dibaryon states of interest here. The lowest (without taking tensor coupling into account) channel for each SIJ is identified by a bold lettering; sc and cc denote single channel (the lowest one) and coupled channels, respectively.

Table III : Masses of Six-Quark Systems with Strangeness

S	I,J	coupling channels	Mass _{sc}	Mass _{cc}
-2	0, 0	$\Lambda\Lambda - N\Xi - \Sigma\Sigma - \Sigma^*\Sigma^*$	2228.8	2224.1
-3	1/2, 2	$N\Omega - \Sigma\Xi^* - \Xi\Sigma^* - \Xi^*\Lambda - \Xi^*\Sigma^*$	2562.0	2549.8
	1/2, 1	$\Lambda\Xi - N\Omega - \Lambda\Xi^* - \Xi\Sigma^* - \Sigma^*\Xi^* - \Sigma\Xi^* - \Sigma\Xi$	2465.9	2465.6
-4	1, 0	$\Xi\Xi - \Sigma^*\Omega - \Xi^*\Xi^*$	2702.7	2700.6
	0, 1	$\Xi\Xi - \Lambda\Omega - \Xi\Xi^* - \Xi^*\Xi^*$	2702.2	2702.1
-5	1/2, 0	$\Xi^*\Omega$	3145.6	-
	1/2, 1	$\Xi\Omega - \Xi^*\Omega$	3001.8	3001.7
-6	0, 0	$\Omega\Omega$	3298.2	-

In 1977, Jaffe[23] studied the color-magnetic interaction of the one-gluon exchange potential in the multiquark system and found that the most attractive channel is the flavor singlet with quark content $u^2d^2s^2$. Moreover, the very same symmetry analysis of the chiral boson exchange potential also leads to the same conclusion[22].

However dibaryon physics can be very delicate. The deuteron channel is not a channel with strong attraction in any baryon interaction model. If the deuteron had not been found experimentally, it seems highly unlikely that any model would have been able to predict it to be a stable dibaryon. The H-particle ($SIJ = -200$) is a six quark state consisting mainly of octet-baryons, similar to the deuteron, and we find only a weak attraction in there also in our model. Hence, a qualitative analysis is insufficient to judge whether or not the H-particle is strong interaction stable. Systematically, we find that a strong attraction develops only in decuplet-decuplet channels and a mild attraction in octet-decuplet channels.

Moreover, in the H-particle case, the channel coupling effect may even be more important than the deuteron case. In our calculation, four channels have been taken into account. These are: $\Sigma\Sigma$, $N\Xi$, $\Lambda\Lambda$ and $\Sigma^*\Sigma^*$. The relative motion wave functions of each channel contribution to the H-particle are shown in Fig 1. We find that $\Sigma\Sigma$ channel provides the

largest contribution (43.4%), the $\Lambda\Lambda$ channel is the next largest (36.8%), followed by the $N\Xi$ channel (15.7%); the $\Sigma^*\Sigma^*$ channel has only a minor effect (4.1%). However, according to the analysis by Jaffe, the biggest contribution is $N\Xi$ channel, and the $\Lambda\Lambda$ channel provides the smallest contribution.

The lowest mass we find for the $u^2d^2s^2$ system is 2224.1MeV , which is 7MeV lower than the experimental threshold of $\Lambda\Lambda$ and 3MeV lower than our model threshold. These values are smaller than the rms uncertainty that may be inferred from our fit to the baryon octet and decuplet in Table II. Furthermore, they are on the order of corrections one would expect from isospin violations which we have not included. Hence, it is not clear whether or not the H particle is strong interaction stable in our model and we consider this to be consistent with recent experimental findings[37].

Besides the binding energy of the H , an interesting question regarding the H is its compactness, i.e., whether the H is a compact 6-quark object or a loosely bound $\Lambda\Lambda$ state. Fig.1 indicates that the maxima of the relative motion wave functions occur around 0.6 fm, and the delocalization parameter, ϵ , of the dominant channel at the maximum is as large as 0.8; hence, the H is a compact six quark system in our model.

With respect to systems with strangeness $S = -3$, we have calculated the state $N\Omega$ ($SIJ=-3,1/2,2$), which was shown to be mildly attractive, with energy below $\Lambda\Xi\pi$ threshold[29]. That conclusion was challenged by Oka[38] and supported by Silvestre-Brac and Leandri[39].

We have carried out a dynamical channel coupling calculation to examine this state further. The $N\Omega, \Lambda\Xi^*, \Xi\Sigma^*, \Sigma\Xi^*, \Xi^*\Sigma^*$ channels are all included. We find the eigen energy to be 2549.8 MeV , $24(54)\text{MeV}$ lower than the $\Lambda\Xi\pi$ experimental(model) threshold. Relative motion cluster wave functions for the individual channels are shown in Fig. 2. The $N\Omega$ channel is by far the dominant one (83.1%) and the maximum for its relative motion wave function occurs at around 0.8 fm. Mixing into the other channels is small. Hence, this is also a compact six quark state. Note that the D-wave $\Lambda\Xi$ and $\Sigma\Xi$ channels have not been included since no tensor interaction has been included in this calculation. This coupling should further affect the eigen energy of the $N\Omega$ ($SIJ=-3,1/2,2$) state and determines the D-wave decay widths to $\Lambda\Xi$ and $\Sigma\Xi$ final states.

We have also calculated the state $SIJ = -3, 1/2, 1$. The lowest eigen energy, 2465.6MeV , is about $32(2)\text{MeV}$ higher than the experimental (model) $\Lambda\Xi$ threshold. The result is almost unchanged by taking into account all possible coupling channels. It is quite possibly a "fall

apart" state.

For systems with $S=-4$, we take the quantum numbers $SIJ = -4, 1, 0$ as an example, because this case bears a number of similarities to the deuteron. For example, in both cases, the lowest mass channel is composed of two octet baryons from the same isodoublet. Also, the matrix element P_{36}^{sfc} characterizing the symmetry property of the system is $-1/81$ for both cases. (P_{36}^{sfc} is the permutation operator of the quarks between two clusters acting in flavor, spin and color space.) We find that the mass to be 2700.6MeV , which is very close to the model threshold of $\Xi\Xi$, but is 65MeV higher than the experimental threshold. Taking into account the $\Xi^*\Xi^*$ and $\Sigma^*\Omega$ channel coupling, binds the system a little more tightly than without channel coupling. This provides yet another example of our earlier contention that it is hard to predict whether or not dibaryons composed of octet baryons are strong interaction stable, because the binding energy is generally small compared to the model uncertainty. We tentatively conclude that the $SIJ = -4, 1, 0$ is also a "fall apart" state.

For comparison, we have also calculated the $SIJ = -4, 0, 1$ state as shown in Table III. The $\Xi\Xi$, $\Xi\Xi^*$, $\Lambda\Omega$ and $\Xi^*\Xi^*$ coupling channels are included. The lowest eigen energy, 2702.1MeV , is a little higher than the mass of $SIJ = -4, 1, 0$. Again we tentatively conclude that this is a "fall apart" state, similar to the $SIJ = -4, 1, 0$.

For the system with $S=-5$, we take the $SIJ = -5, 1/2, 0$ state as an example. This state is interesting due to its $\langle P_{36}^{sfc} \rangle$ value, $\sim -1/9$, which makes it a Pauli principle favored state. If only two-baryon S-wave channels are taken into account, there is only one channel for this state. Our calculation shows that the contribution of the kinetic energy term, due to quark exchange and delocalization effects, contributes strongly towards the formation of a bound state. However, the one-gluon-exchange interaction largely compensates for this attraction and produces a mass of 3145.6MeV , which is 59MeV lower than the experimental value of the $\Xi^*\Omega$ threshold but only about 2MeV lower than the model threshold. (The one-gluon-exchange effect here is quite different from that in the d^* case, where large delocalization is favored for a wide range of cluster separations as well as there being a strong effective attraction due to the large reduction in the kinetic energy that accompanies significant delocalization.) We conclude that this state is not a good candidate for a dibaryon resonance search due to its small binding and its $\Xi^*\Omega$ content.

Inclusion of the tensor interaction will mix the spin-2 D-wave $\Xi\Omega$ channel with the spin-0 S-wave $\Xi^*\Omega$ channel. The effect of the tensor coupling on the $SIJ = -5, 1/2, 0$ state would therefore be interesting to calculate.

In the same strangeness sector, we also calculated the $SIJ = -5, 1/2, 1$ state, since it includes the lowest channel, $\Xi\Omega$. We find a mass of 3001.7MeV , about 144MeV lower than that of the $SIJ = -5, 1/2, 0$ state, but about $12(2)\text{MeV}$ higher than the experimental (model) threshold of $\Xi\Omega$. Again, it is possibly a "fall apart" state.

IV. DISCUSSION

Our model results for the binding energy of high strangeness dibaryons are systematically smaller than those of the chiral quark model[36]. The difference is mainly due to the different mechanism for the origin of the effective BB intermediate range attraction.

In the chiral quark model[8, 9, 36] the intermediate range attraction is attributed to σ meson exchange. Because of its scalar-isoscalar character, σ meson exchange provides a universal attraction independent of the flavor. If the exchange of σ mesons is an effective description of correlated two π exchange, as discussed in the Yukawa meson-baryon coupling model, then it would be impossible to extend it directly from the NN channel to channels with strangeness. For example, in the NN channel, there are NN, $N\Delta$ and $\Delta\Delta$ intermediate states, while for the $\Lambda\Lambda$ channel, there is only the $\Sigma\Sigma$ intermediate state, and for the $\Xi\Xi$ and $\Omega\Omega$ channels, no intermediate state is possible. Therefore it is unreliable to fix the parameters for the σ exchange from the NN channel and then directly extend that exchange to channels with strangeness.

There are arguments based on spontaneous chiral symmetry breaking for introduction of the σ meson quark coupling. In the SU(2) case, the non-linear realization of chiral symmetry can be linearized and in turn the σ and π meson coupling constants can be unified[7, 8]. In the SU(3) case also, one can introduce SU(3) chiral symmetry by neglecting the s quark mass, followed by spontaneous symmetry breaking. However, the nonlinear realization of SU(3) can not be linearized in the same way as in the SU(2) case to obtain the σ . Hence, a strong attraction in high strangeness channels arising due to a universal σ quark coupling must be treated as a model dependent result that requires further study.

In the QDCSM, the intermediate range attraction is mainly due to reduction of the quark

kinetic energy. In Figs.3-10, we show the contributions of the kinetic energy, confinement, color Coulomb, and color magnetic terms to the effective BB interaction, as well as the total sum, in curves a-e, respectively, for few typical channels. The contribution of π exchange with a cut-off $r_0 = 0.8 fm$ is small so we do not show it. These figures are ordered in terms of increasing values of $\langle P_{36}^{sfc} \rangle$, from Pauli favored to forbidden.

Quark exchange alone induces a weak reduction in kinetic energy. Quark delocalization enhances this kinetic energy reduction. The kinetic energy reduction is also dependent on the strangeness of the channels due to the inverse quark mass dependence of the quark kinetic energy. The higher the strangeness, the smaller the contribution of quark kinetic energy and hence the less the reduction of the kinetic energy due to delocalization (see Figs.3-10(a)). This makes the intermediate range attraction weaker for the higher strangeness channels and is the main reason that our model gives less binding for the $S = -4, -5, -6$ states than does the chiral quark model[36].

If the usual quadratic color confinement is used, it does not contribute to the effective BB interaction. After introducing quark delocalization, the usual color confinement will contribute an effective repulsion, as shown in Fig.11. The color Coulomb has a similar behavior, as shown in Fig.3-10(c); it almost does not contribute to the effective BB interaction without quark delocalization, and contributes an effective repulsion with quark delocalization. These two terms working together almost totally forbid quark delocalization. This implies that the internal structure of the baryon is unaffected by this interaction but that is inconsistent with the observed difference between the average nucleon structure function in a nucleus and in isolation as seen in deep inelastic lepton scattering (EMC effect).

On the other hand, there is no compelling reason to assume that the two body confinement potential is a good approximation for a multi-quark system. At the very least, the three gluon and the three body instanton interactions, which do not contribute to the $q\bar{q}$ meson and q^3 baryon but do contribute to the multi-quark system, have been omitted in the two body confinement model. To take these facts into account, the QDCSM reparametrizes the confinement by introducing color screening[10, 11, 12, 15, 26, 28]. Figs.3-10(b) show that after the introduction of color screening, the confinement term contributes an additional attraction, which mainly reduces the repulsive core of the effective BB interactions. We recognize that there is a model uncertainty related to this term.

The color magnetic term generally contributes to a repulsive core except for a few Pauli

favored channels where it contributes an additional intermediate range attraction so that these channels develop a strong total attraction. It is also dependent on the strangeness of the channels: The higher the channel strangeness, the weaker the color magnetic contribution, due to the inverse strange quark mass in the color magnetic term. Figs.3-10(d) display these results.

Together, these figures show that the quark delocalization is determined by the competition of these four terms and that the competition is different in different channels. We have mentioned before that in the d^* channel this competition produces a large quark delocalization for a wide range of separations between two Δ -like quark clusters so that the kinetic energy acquires a correspondingly large reduction, giving rise to a very strong attraction in this channel. (See Fig.3). The $SIJ = -6, 0, 0$ and $-5, 1/2, 0$ channels have a similar opportunity to develop large quark delocalizations and strong attraction. However, there the competition did not allow a large quark delocalization to develop and so the resulting attraction is not as strong as in the d^* channel. (See Figs.4-5.)

V. CONCLUSION

In our model, the QDCSM, it is the quark dynamics that controls the competition among the four terms and determines the final effective BB interactions which are quite similar, though not identical, to those of the quark-gluon-meson hybrid model[14] for the majority of BB channels. In view of the fact that the H particle has not been observed experimentally, the BB interaction in the $\Lambda\Lambda$ channel[37] may be more accurate than in some other models. We also obtain agreement with the properties of the deuteron and the existing NN, $N\Lambda$ and $N\Sigma$ scattering data. Further refinement is possible by including more channel couplings and the spin-orbit and tensor interactions. Of course the QDCSM is only a model of QCD. The high strangeness dibaryon resonances may be a good venue for determining whether the QDCSM mechanism for the intermediate range attraction is more accurate than that of the meson exchange models.

To sum up, we have carried out a dynamical calculation for the most promising dibaryon candidates with high strangeness by using the extended QDCSM. Our calculation recommends only a few high strangeness states as worthy of being searched for experimentally. These are the H particle, an $N\Omega$ and the di- Ω . The di- Ω was previously reported in Ref.([35])

and the result has been included in Table III.

The H particle and the di- Ω may be strong interaction stable. However in our model, the binding energies of both are small relative to the model uncertainty. The di- Ω mass is about $47MeV$ lower than the experimental $\Omega\Omega$ threshold. However our model mass for the Ω is $1650MeV$. If this model mass of Ω were used to calculate the threshold, then the di- Ω mass is no more than $2MeV$ below that threshold. Since our model mass for the single Ω baryon deviates from the experimental value about $22MeV$, a reasonable estimate of the model uncertainty for the dibaryon would be at least that large. Therefore the di- Ω should not be claimed as a strong interaction stable dibaryon within the model. Similarly, we cannot claim that the H particle is strong interaction stable either. The $SIJ = -3, 1/2, 2$ $N\Omega$ case is certainly not strong interaction stable. However, the state is also certainly lower in mass than the $N\Omega$ threshold, and quite possibly lower than the $\Lambda\Xi\pi$ threshold, too. This strongly suggests that it is a promising candidate for a dibaryon resonance. Unfortunately, a check of this possibility by means of $\Lambda\Xi$ scattering cannot be expected to occur in the near future.

This work is supported by the NSFC contract 90103018 and by the U.S. Department of Energy under contract W-7405-ENG-36. F. Wang would like to thank the ITP for their support through the visiting program.

[1] R.T. Cahill and C.D. Roberts, Phys. Rev. **D32**, 2419 (1985).

[2] P.C. Tandy, Prog. Part. Nucl. Phys. **39**, 117 (1997).

R.T. Cahill and S.M. Gunner, Fizika **B7**, 17 (1998).

X.F. Lu, Y.X. Liu, H.S. Zong and E.G. Zhao, Phys. Rev. **C58**, 1195 (1998).

[3] C.D. Roberts and S.M. Schmidt, Prog. Part. Nucl. Phys. **45S1**, 1-103 (2000).

[4] A. De Rúujula, H. Georgi and S.L. Glashow, Phys. Rev. **D12**, 147 (1975).

[5] N. Isgur and G. Karl, Phys. Rev. **D18**, 4187 (1978); **D19**, 2653 (1979); **D20**, 1191 (1979).

[6] A. Faessler and F. Fernandez, Phys. Lett. **B124**, 145 (1983).

[7] I.T. Obukhovsky and A.M. Kusainov, Phys. Lett. **B238**, 142 (1990).

[8] F. Fernandez, A. Valcarce, U. Straub and Z. Faessler, J. Phys. **G19**, 2013 (1993).

[9] Y. Fujiwara, C. Nakamoto and Y. Suzuki, Phys. Rev. Lett. **76**, 2242 (1996).

Y. Fujiwara, T. Fujita, M. Kohno, C. Nakamoto, and Y. Suzuki, Phys. Rev. **C65**, 014002

(2002).

- [10] F. Wang, G.H. Wu, L.J. Teng and T. Goldman, Phys. Rev. Lett. **69**, 2901 (1992).
- [11] G. Wu, L. Teng, J.L. Ping, F. Wang and T. Goldman, Phys. Rev. **C53**, 1161 (1996).
- [12] G.H. Wu, J.L. Ping, F. Wang and T. Goldman, Nucl. Phys. **A673**, 279 (2000).
- [13] J. Ping, F. Wang and T. Goldman, Phys. Rev. **C62**, 054007 (2000).
- [14] H.R. Pang, J.L. Ping, F. Wang and T. Goldman, Phys. Rev. **C65**, 014003 (2001).
- [15] J. Ping, H. Pang, F. Wang and T. Goldman, Phys. Rev. **C65**, 044003 (2002).
- [16] X.F. Lu, J.L. Ping and F. Wang, Chin. Phys. Lett. **20**, 42 (2003).
- [17] L.Ya. Glozman, et al., Phys. Rev. **C57**, 3406 (1998); Nucl. Phys. **A663-664**, 103c (2000); nucl-th/9909021.
- [18] K.F. Liu et al., Phys. Rev. **D59**, 112001 (1999); Phys. Rev. **D61**, 118502 (2000).
- [19] N. Isgur, Phys. Rev. **D61**, 118501; **D62**, 054026 (2000).
- [20] H. Collins and H. Georgi, Phys. Rev. **D59**, 094010 (1999).
- [21] A. Valcarce, P. Gonzalez, F. Fernandez and V. Vento, Phys. Rev. **C61**, 019803 (2000); H. Garcilazo, A. Valcarce and F. Fernandez, Phys. Rev. **C63**, 035207 (2001); C. Nakamoto and H. Toki, Prog. Theor. Phys. **99**, 1001 (1998).
- [22] F. Wang, J.L. Ping, H.R. Pang and T. Goldman, Mod. Phys. Lett. **A18**, 356 (2003); nucl-th/0212012.
- [23] R.L. Jaffe, Phys. Rev. Lett. **38**, 195 (1977).
- [24] R. Bilger, et al., Phys. Rev. Lett. **71**, 42 (1993); **72**, 2972 (1994); Phys. Lett. **B420**, 37 (1998); **B428**, 18 (1998); **B443**, 77 (1998); K. Fohl, et al., Phys. Rev. Lett. **79**, 3849 (1997); J. Grater, et al., Phys. Rev. **C58**, 1576 (1998); Nucl. Phys. **A663-664**, 469c (2000); F. Hinterberger et al., Nucl. Phys. **A663-664**, 533c (2000); W. Brodowski, et al., Phys. Rev. Lett. **88**, 192301 (2002); nucl-ex/0206020; S.M. Kiselev, et al., Nucl. Phys. **A650**, 78 (1999).
- [25] T. Goldman et al., Phys. Rev. **C39**, 1889 (1989).
- [26] F. Wang et al., Phys. Rev. **C51**, 3411 (1995).
J.L. Ping, F. Wang and T. Goldman, Nucl. Phys. **A657**, 95 (1999).
- [27] T. Goldman, et al., Mod. Phys. Lett. **A13**, 59 (1998).
- [28] J.L. Ping, F. Wang and T. Goldman, Nucl. Phys. **A688**, 871 (2001).
- [29] T. Goldman et al., Phys. Rev. Lett. **59**, 627 (1987).

- [30] V.B. Kopeliovich, Nucl. Phys. **A639**, 75c (1998).
- [31] Z.Y. Zhang, Y.W. Yu, C.R. Ching, T.H. Ho and Z.D. Lu, Phys. Rev. **C61**, 065204 (2000).
- [32] P. LaFrance and E.L. Lomon, Phys. Rev. **D34**, 1341 (1986) and references therein.
- [33] F. Lehar, in: Baryons'98, ed. D.W. Menze and B.Ch. Metsch, (World Scientific, Singapore, 1999) p.622.
- [34] A.J. Buchmann, Y. Yamauchi and A. Faessler, Nucl. Phys. **A496**, 621 (1989).
- [35] H. Pang, J. Ping, F. Wang and T. Goldman, Commun. Theor. Phys. **38**, 424 (2002); Phys. Rev. **C66**, 025201 (2002).
- [36] Q.B. Li, P.N. Shen, Z.Y. Zhang and Y.W. Yu, Nucl. Phys. **A683**, 487 (2001).
- [37] H. Takahashi et al., Phys. Rev. Lett. **87**, 212502 (2002).
- [38] M. Oka, Phys. Rev. **D38**, 298 (1988).
- [39] B. Silvestre-Brac and J. Leandri, Phys. Rev. **D45**, 4221 (1992).

FIGURE CAPTIONS

Fig.1 Relative motion wave functions of the coupled channels for the $SIJ=-2,0,0$ state with eigen energy 2224.1 MeV.

Fig.2 Relative motion wavefunctions of the coupled channels for the $SIJ=-3,1/2,2$ state with eigen energy 2549.8 MeV.

Fig.3 Contributions of kinetic energy, confinement, color Coulomb and color magnetic terms (a-d respectively) to the effective potential and the total (e) for the $SIJ=0,0,3$ $\Delta\Delta$ channel with $P_{36}^{sfc} = -1/9$. In each subfigure, the dotted curve is for delocalization parameter $\epsilon=0.0$, dashed curve for $\epsilon=0.5$, dashed-dotted curve for $\epsilon = 1.0$; the solid curve is for the self-consistent value of ϵ determined by the system dynamics.

Fig.4 The same as Fig.3 for the state $SIJ = -6, 0, 0$ $\Omega\Omega$ with $\langle P_{36}^{sfc} \rangle = -1/9$.

Fig.5 The same as Fig.3 for the state $SIJ = -5, 1/2, 0$ $\Xi^*\Omega$ with $\langle P_{36}^{sfc} \rangle = -1/9$.

Fig.6 The same as Fig.3 for the state $SIJ = 0, 0, 2$ $\Delta\Delta$ with $\langle P_{36}^{sfc} \rangle = -1/27$.

Fig.7 The same as Fig.3 for the state $SIJ = -3, 1/2, 0$ $\Lambda\Xi$ with $\langle P_{36}^{sfc} \rangle = -1/27$.

Fig.8 The same as Fig.3 for the state $SIJ = 0, 0, 1$ NN with $\langle P_{36}^{sfc} \rangle = -1/81$.

Fig.9 The same as Fig.3 for the state $SIJ = -2, 0, 0$ $\Lambda\Lambda$ with $\langle P_{36}^{sfc} \rangle = 0$.

Fig.10 The same as Fig.3 for the state $SIJ = 0, 1, 1$ NN with $\langle P_{36}^{sfc} \rangle \sim 1/9$.

Fig.11 The contribution of usual quadratic color confinement to the effective BB interaction. The solid curve is for $\epsilon=0.0$, dotted curve for $\epsilon=0.5$ and the dashed curve for $\epsilon=1.0$.

FIG.1

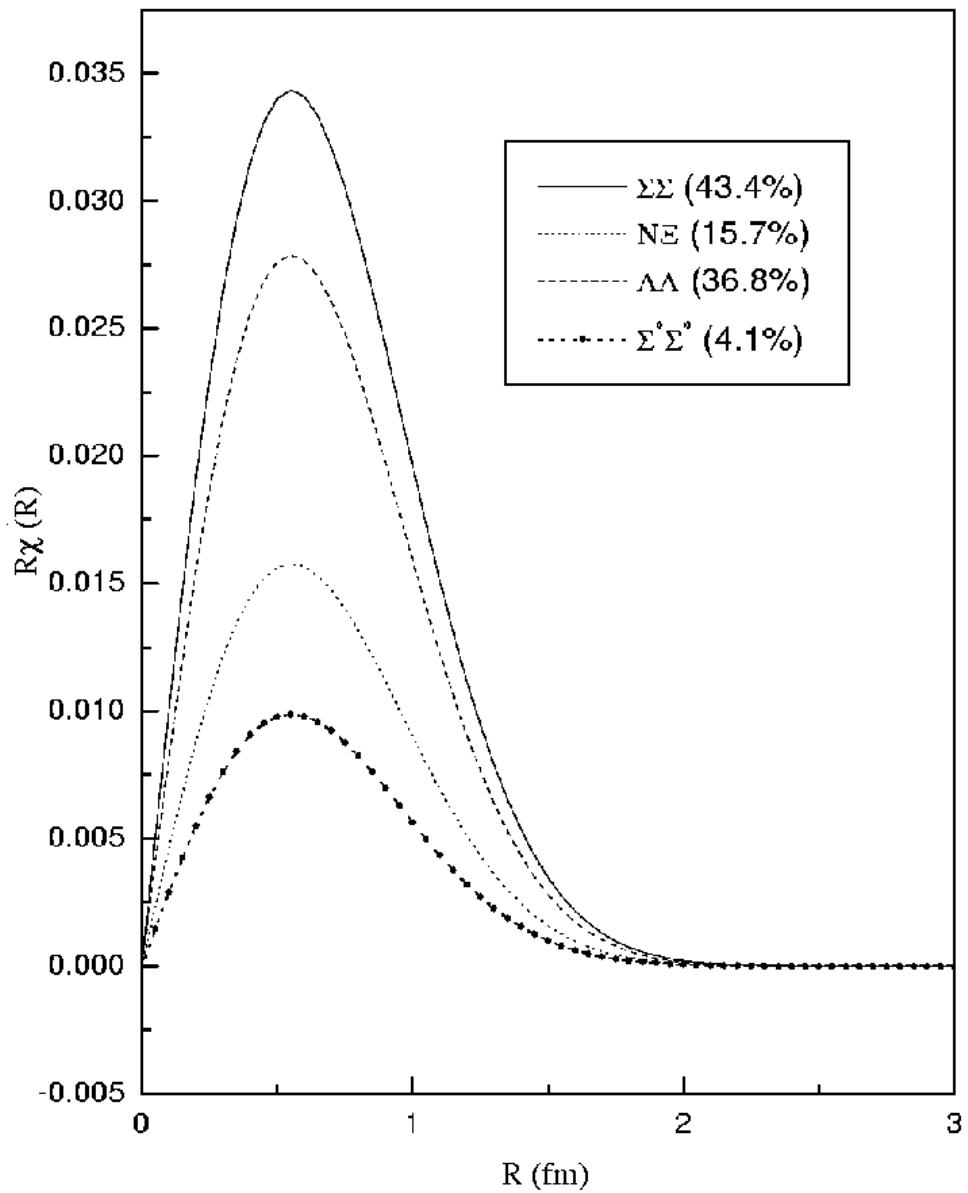


FIG. 1: Relative motion wave functions of the coupled channels for the $SIJ=-2,0,0$ state with eigen energy 2224.1 MeV.

FIG.2

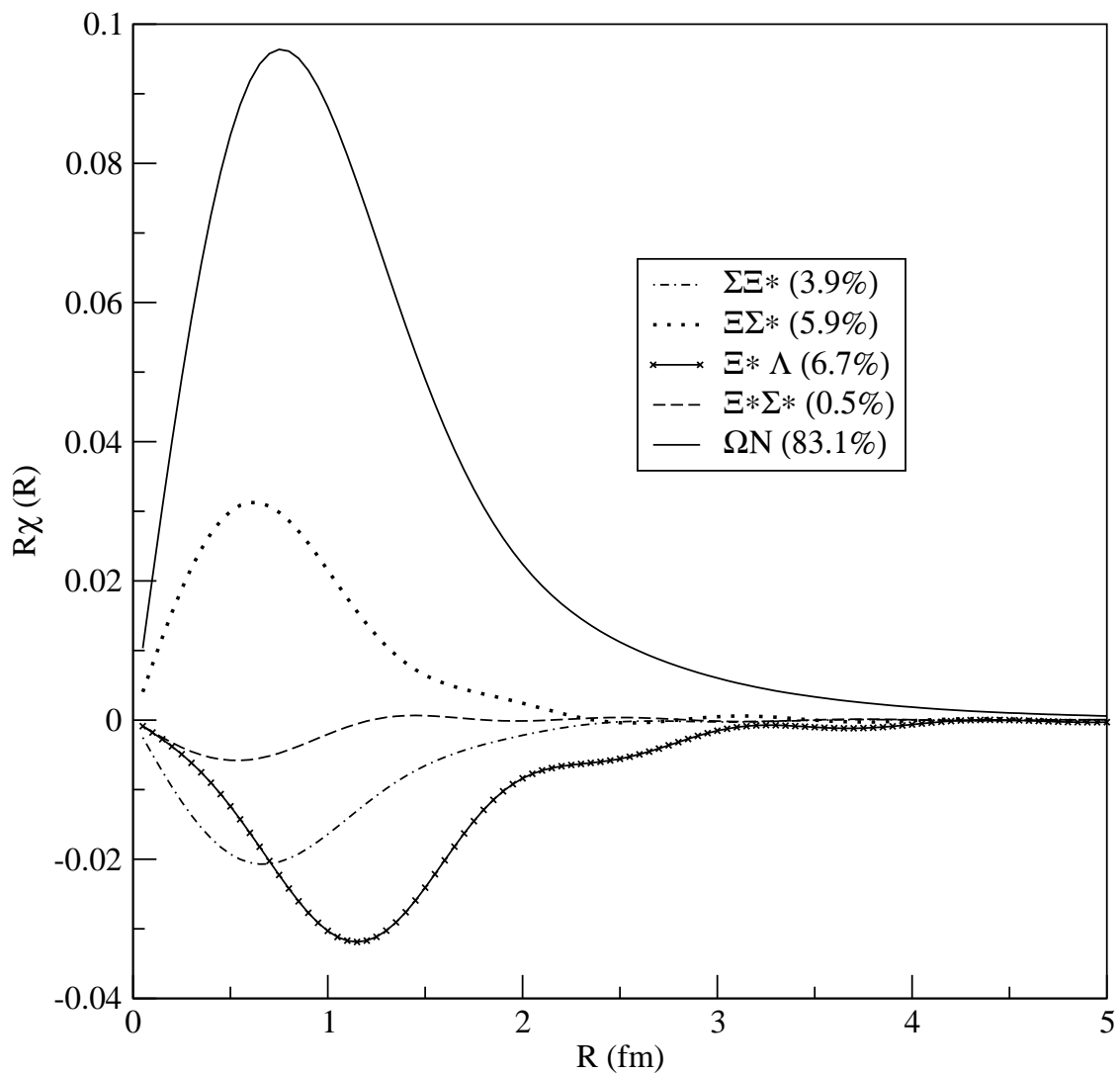


FIG. 2: Relative motion wavefunctions of the coupled channels for the $SIJ=-3,1/2,2$ state with eigen energy 2549.8 MeV.

FIG.3

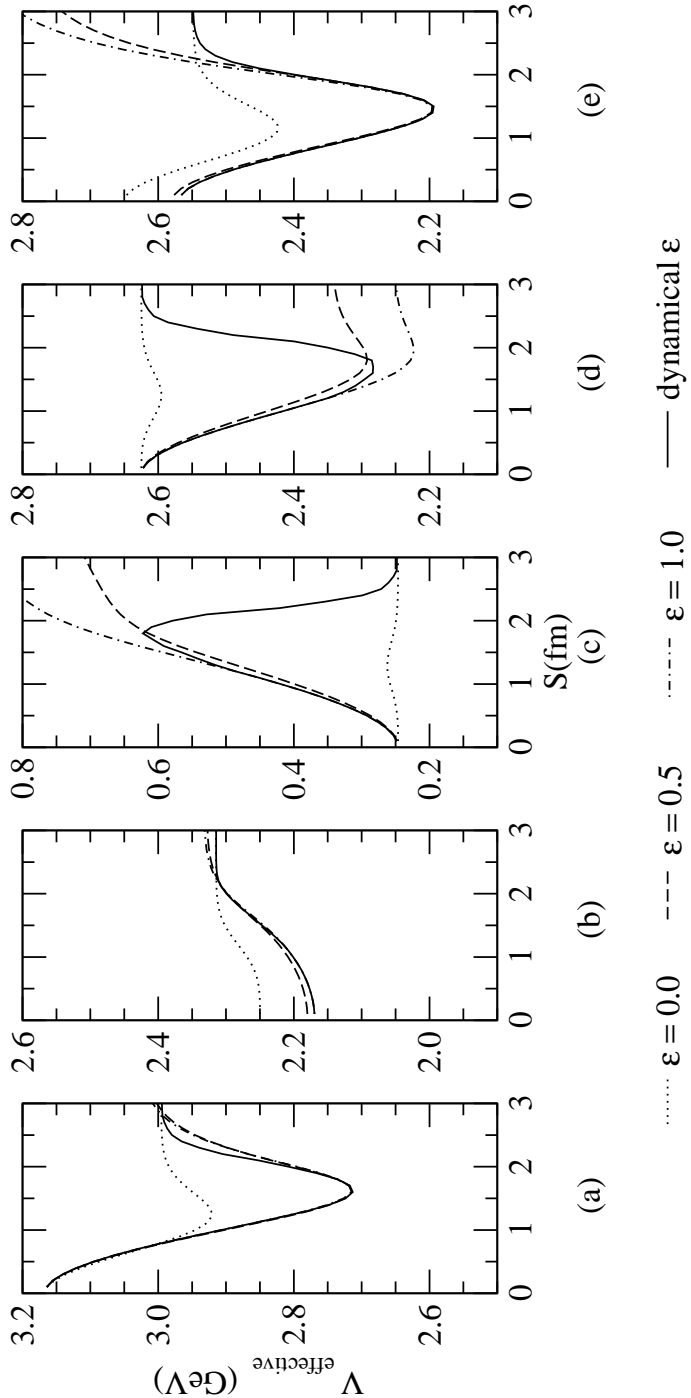


FIG. 3: Contributions of kinetic energy, confinement, color Coulomb and color magnetic terms (a-d respectively) to the effective potential and the total (e) for the SIJ=0,0,3 $\Delta\Delta$ channel with $P_{36}^{sfc} = -1/9$. In each subfigure, the dotted curve is for delocalization parameter $\epsilon=0.0$, dashed curve for $\epsilon=0.5$, dashed-dotted curve for $\epsilon = 1.0$; the solid curve is for the self-consistent value of ϵ determined by the system dynamics.

FIG.4

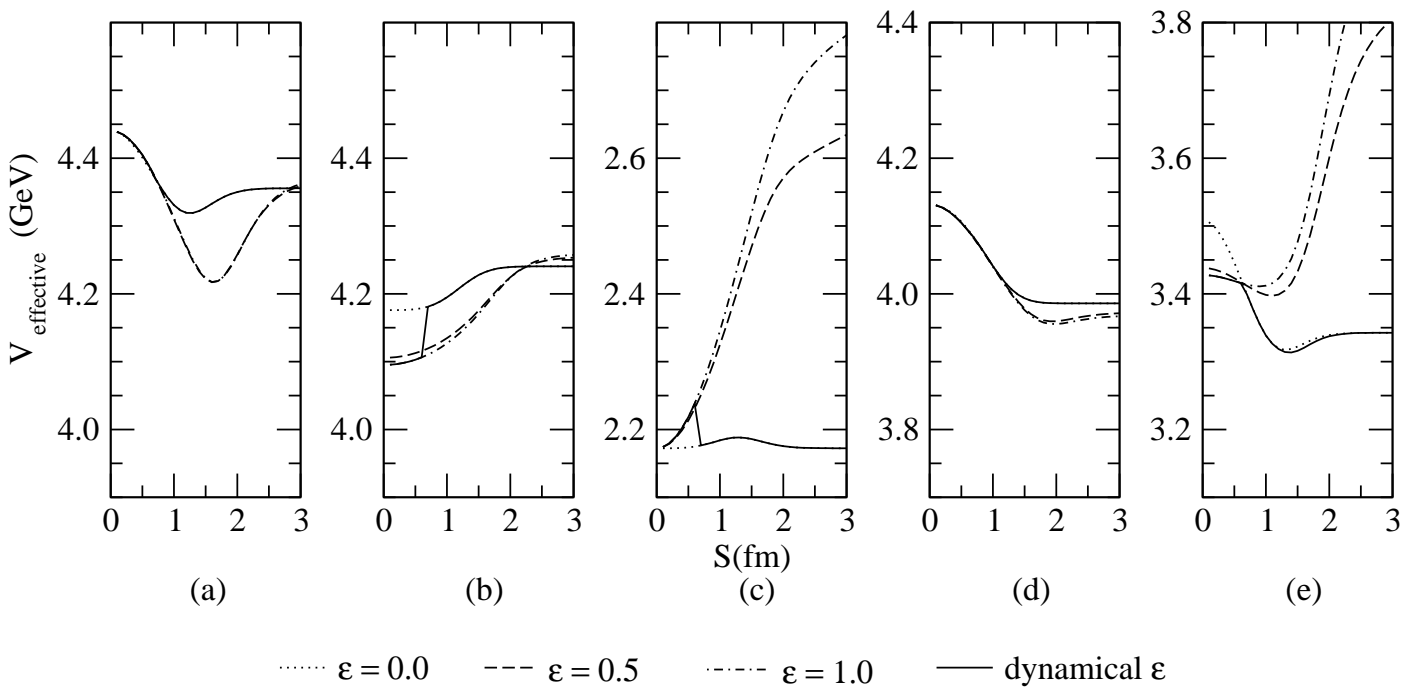


FIG. 4: The same as Fig.3 for the state $SIJ = -6, 0, 0$ $\Omega\Omega$ with $\langle P_{36}^{sf} \rangle = -1/9$.

FIG.5

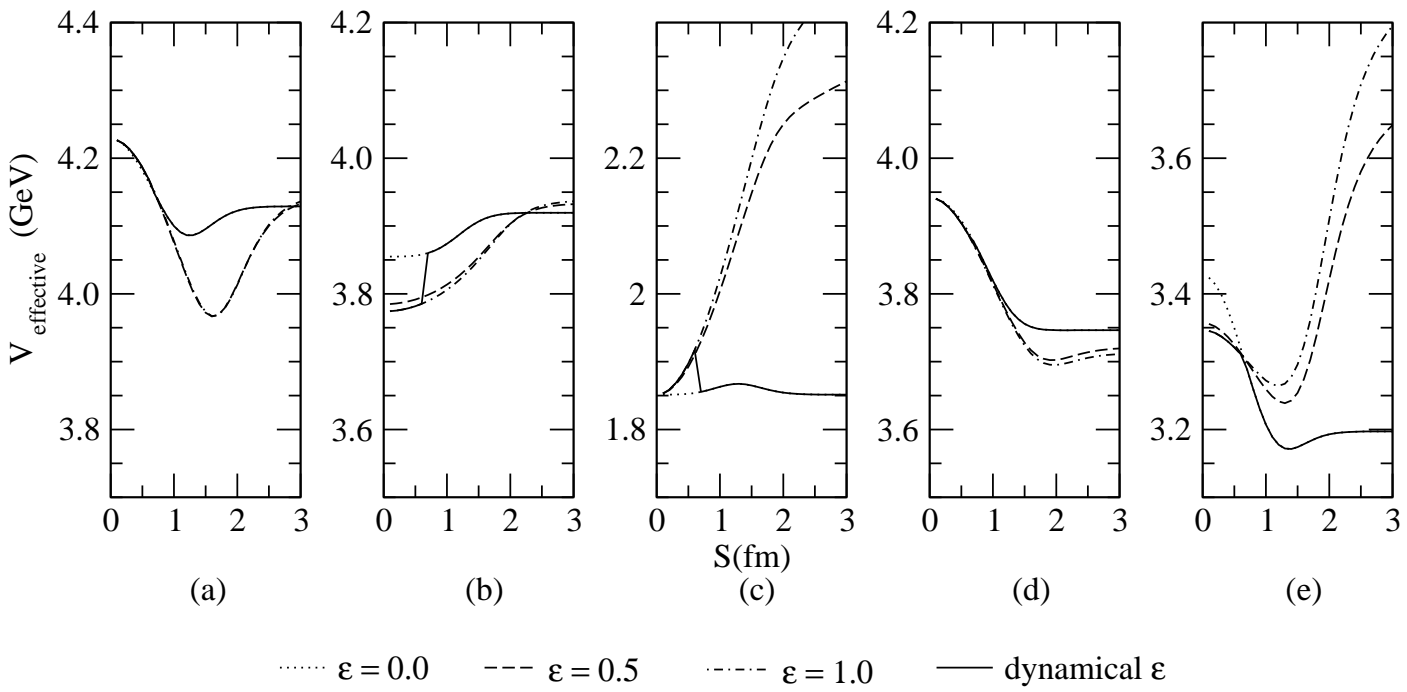


FIG. 5: The same as Fig.3 for the state $SIJ = -5, 1/2, 0$ $\Xi^* \Omega$ with $\langle P_{36}^{sf} \rangle = -1/9$.

FIG.6

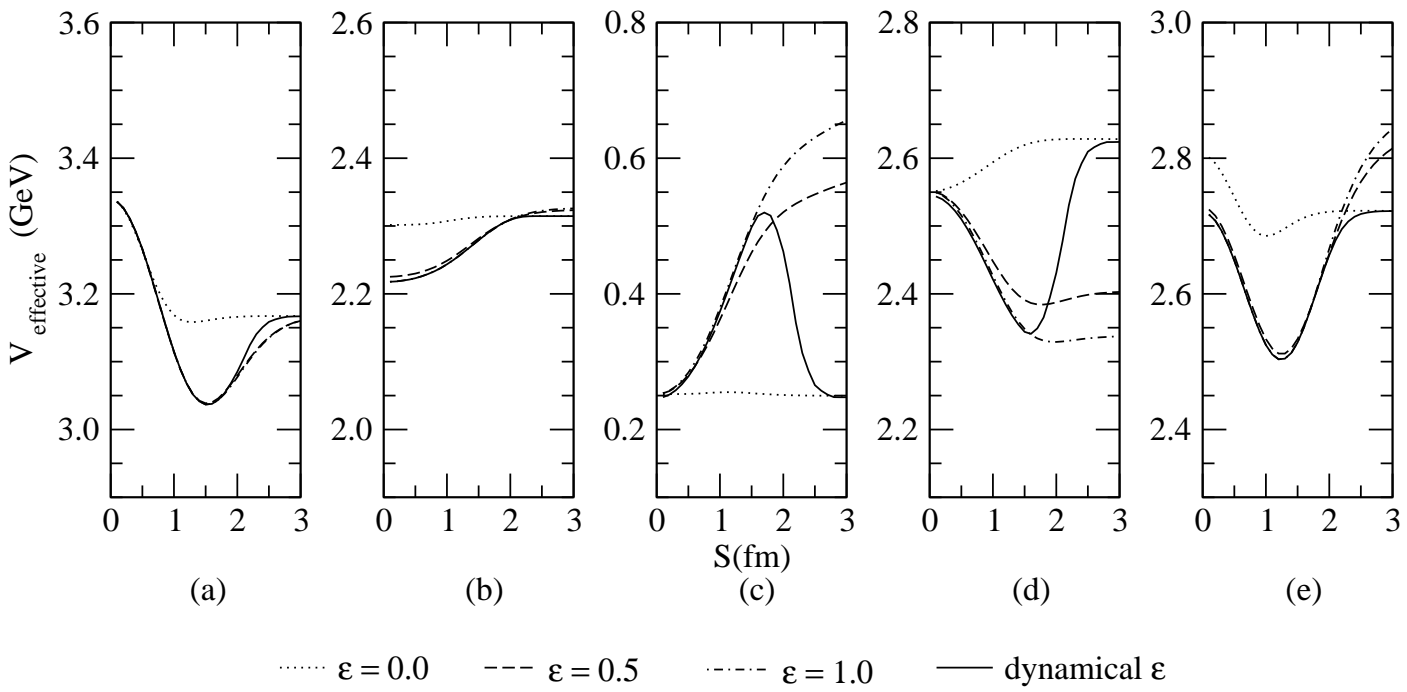


FIG. 6: The same as Fig.3 for the state $SIJ = 0, 0, 2$ $\Delta\Delta$ with $\langle P_{36}^{sf^c} \rangle = -1/27$.

FIG.7

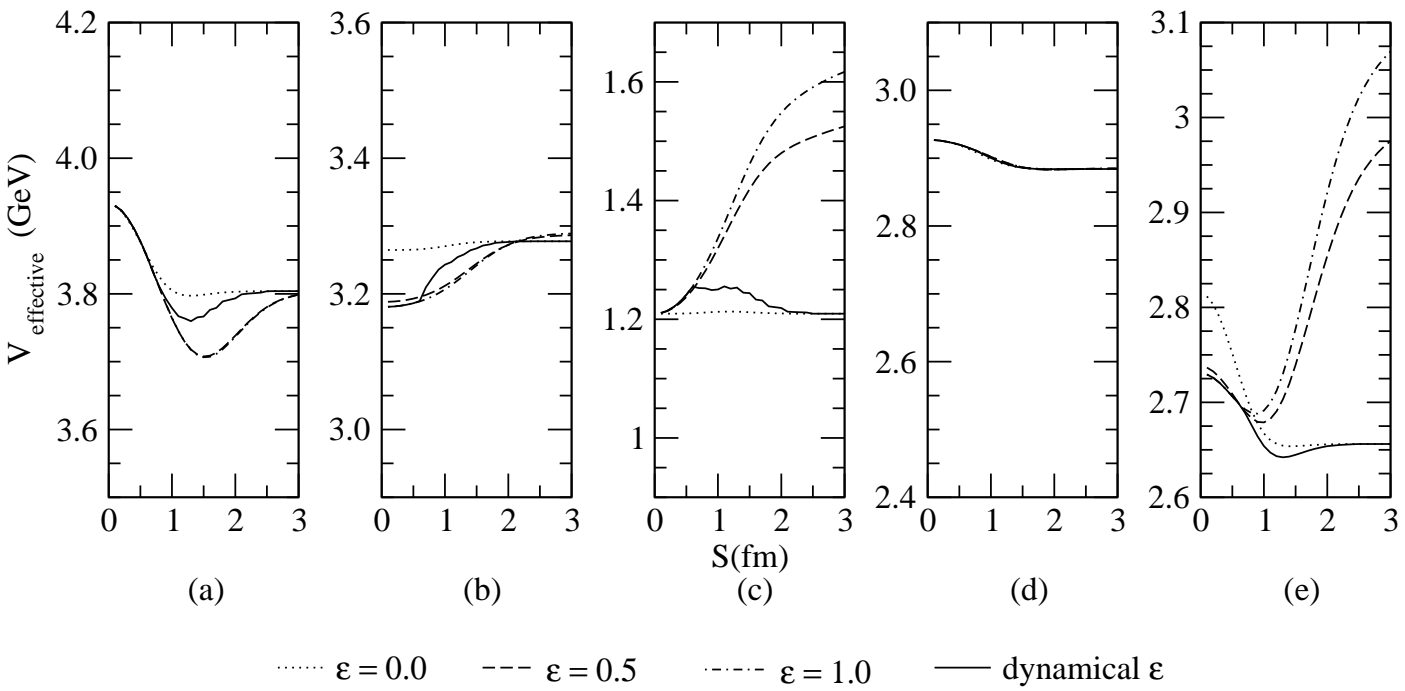


FIG. 7: The same as Fig.3 for the state $SIJ = -3, 1/2, 0$ $\Lambda\Xi$ with $\langle P_{36}^{sf} \rangle = -1/27$.

FIG.8

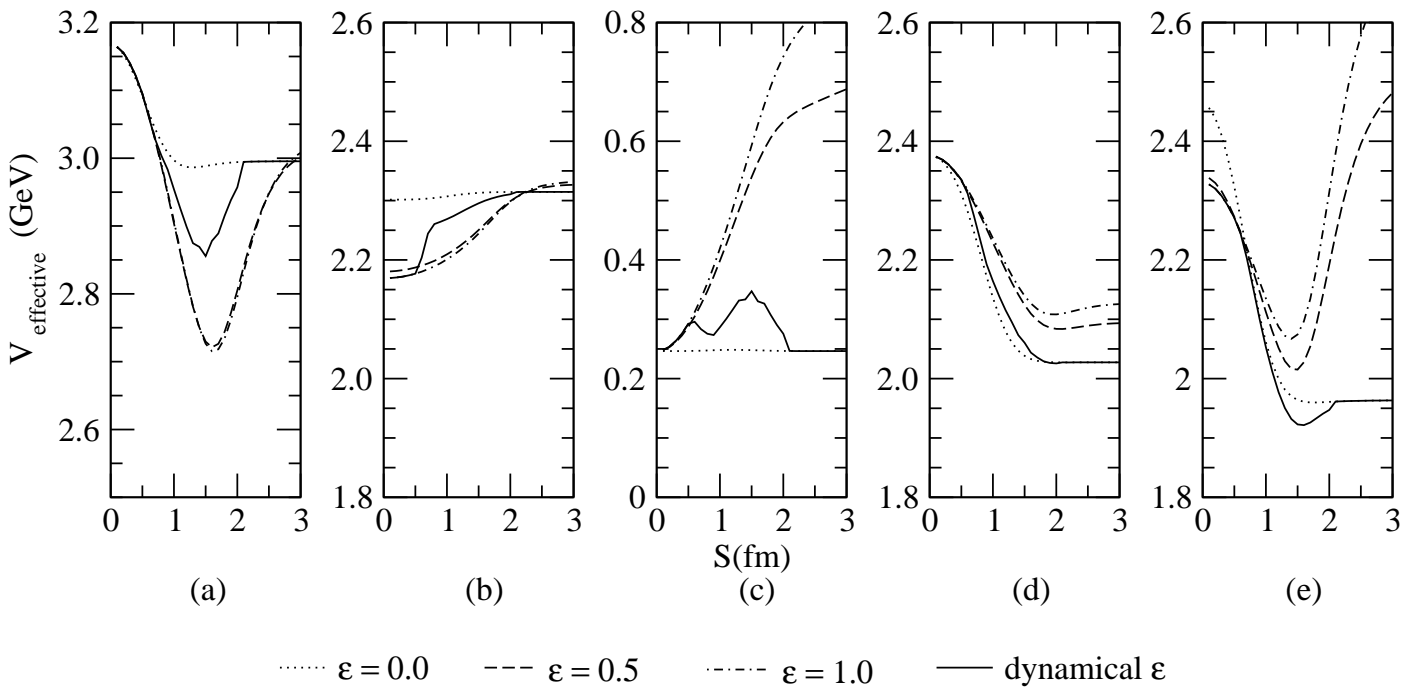


FIG. 8: The same as Fig.3 for the state $SIJ = 0, 0, 1$ NN with $\langle P_{36}^{sf} \rangle = -1/81$.

FIG.9

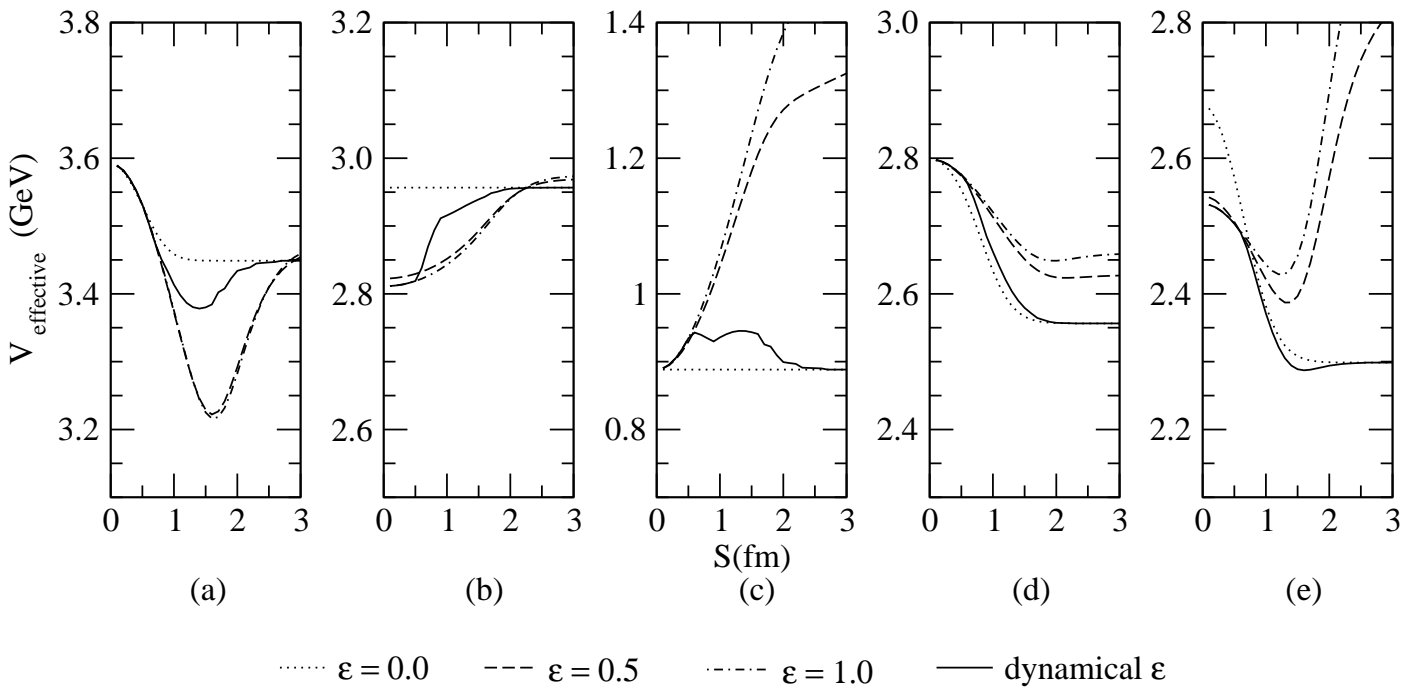


FIG. 9: The same as Fig.3 for the state $SIJ = -2, 0, 0$ $\Lambda\Lambda$ with $\langle P_{36}^{sf} \rangle = 0$.

FIG.10

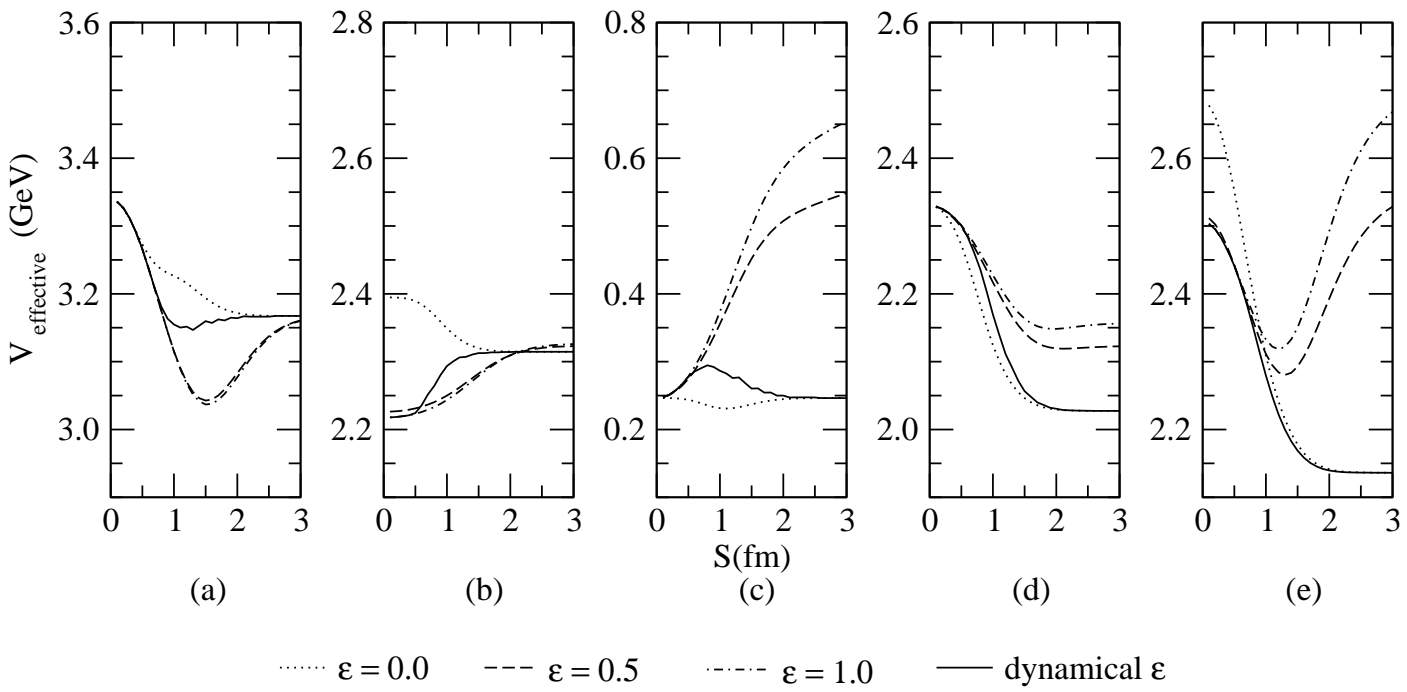


FIG. 10: The same as Fig.3 for the state $SIJ = 0, 1, 1$ NN with with $\langle P_{36}^{sf} \rangle \sim 1/9$.

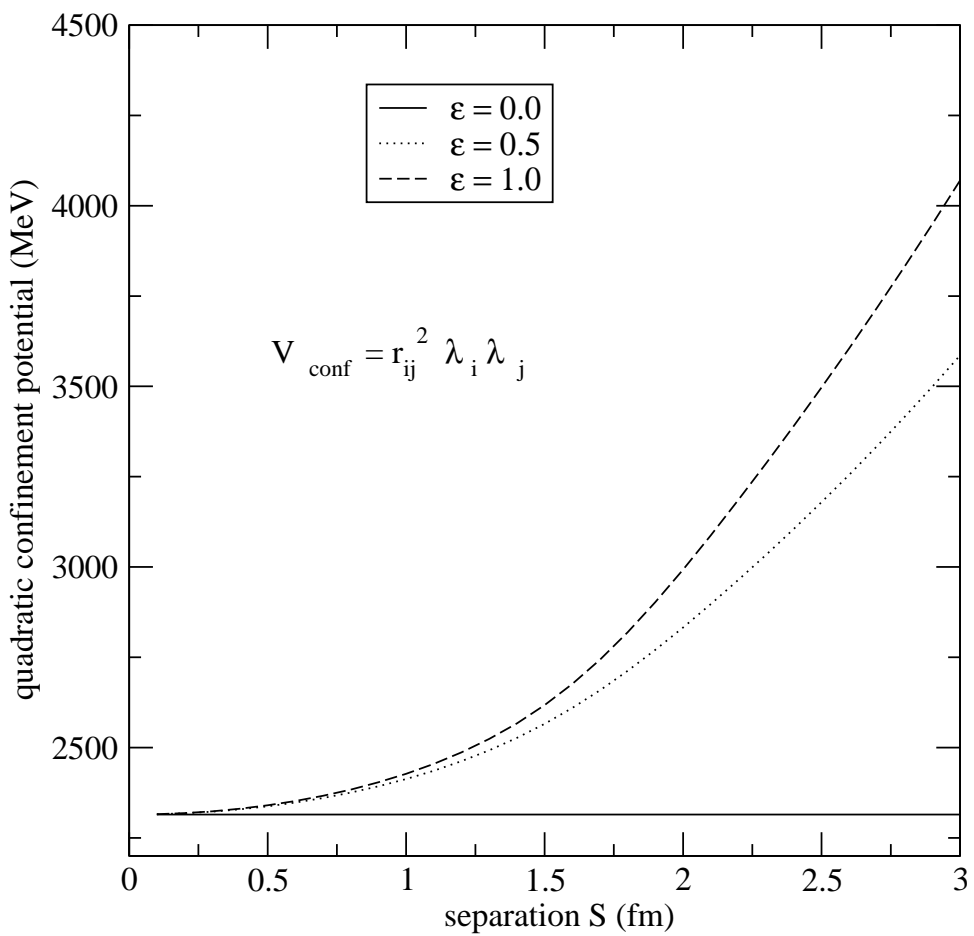


FIG. 11: The contribution of usual quadratic color confinement to the effective BB interaction. The solid curve is for $\epsilon=0.0$, dotted curve for $\epsilon=0.5$ and the dashed curve for $\epsilon=1.0$.